Fig. 4.8. One-dimensional semi-infinite lattice model potential

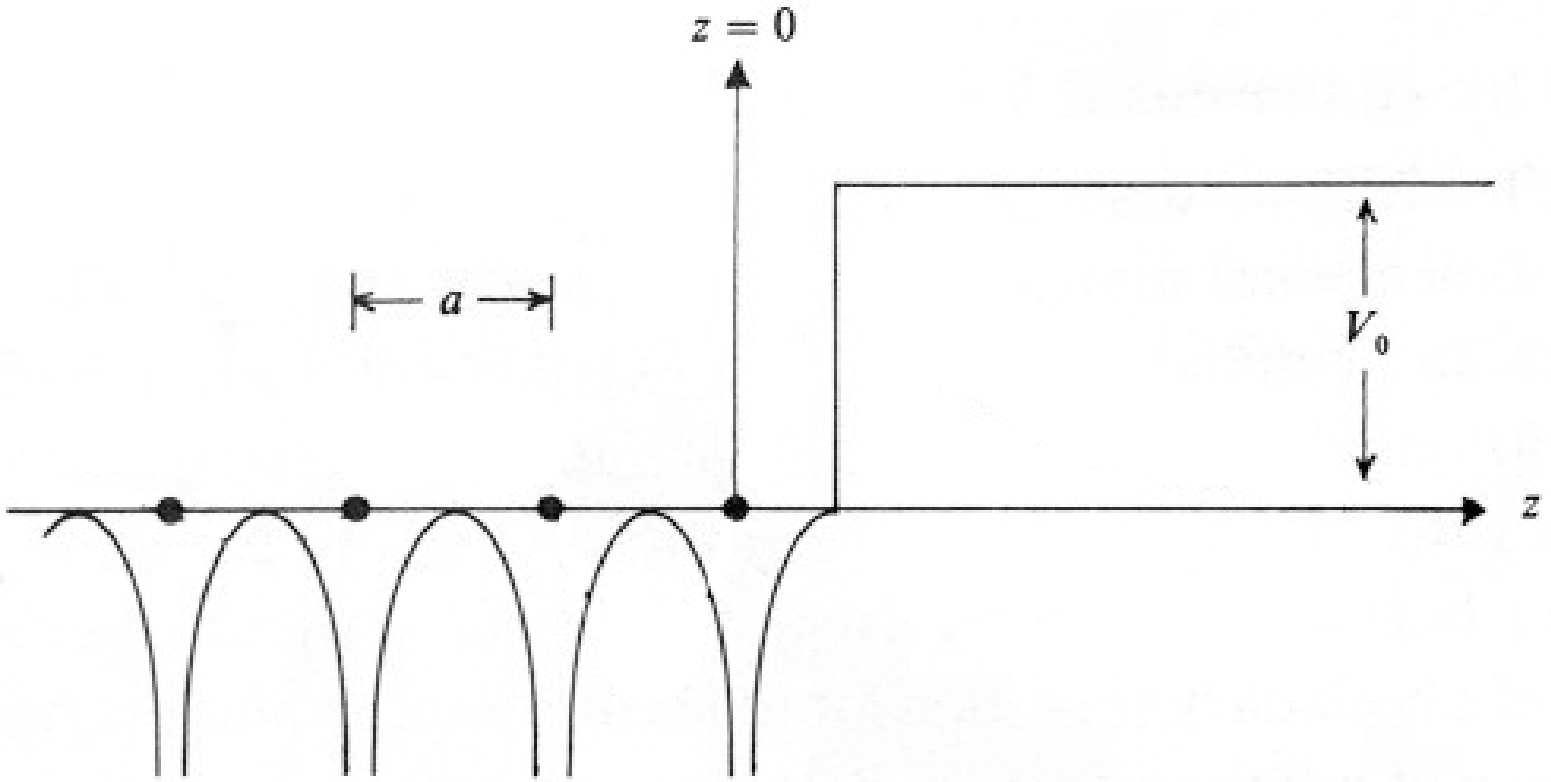

Fig. 4.10. Wave function matching at $z = a/2$: (*a*) $V_g < 0$; (*b*) $V_g > 0$. The sequence 1, 2, 3, indicates increasing energy starting from the bottom of the gap (Forstmann, 1970).

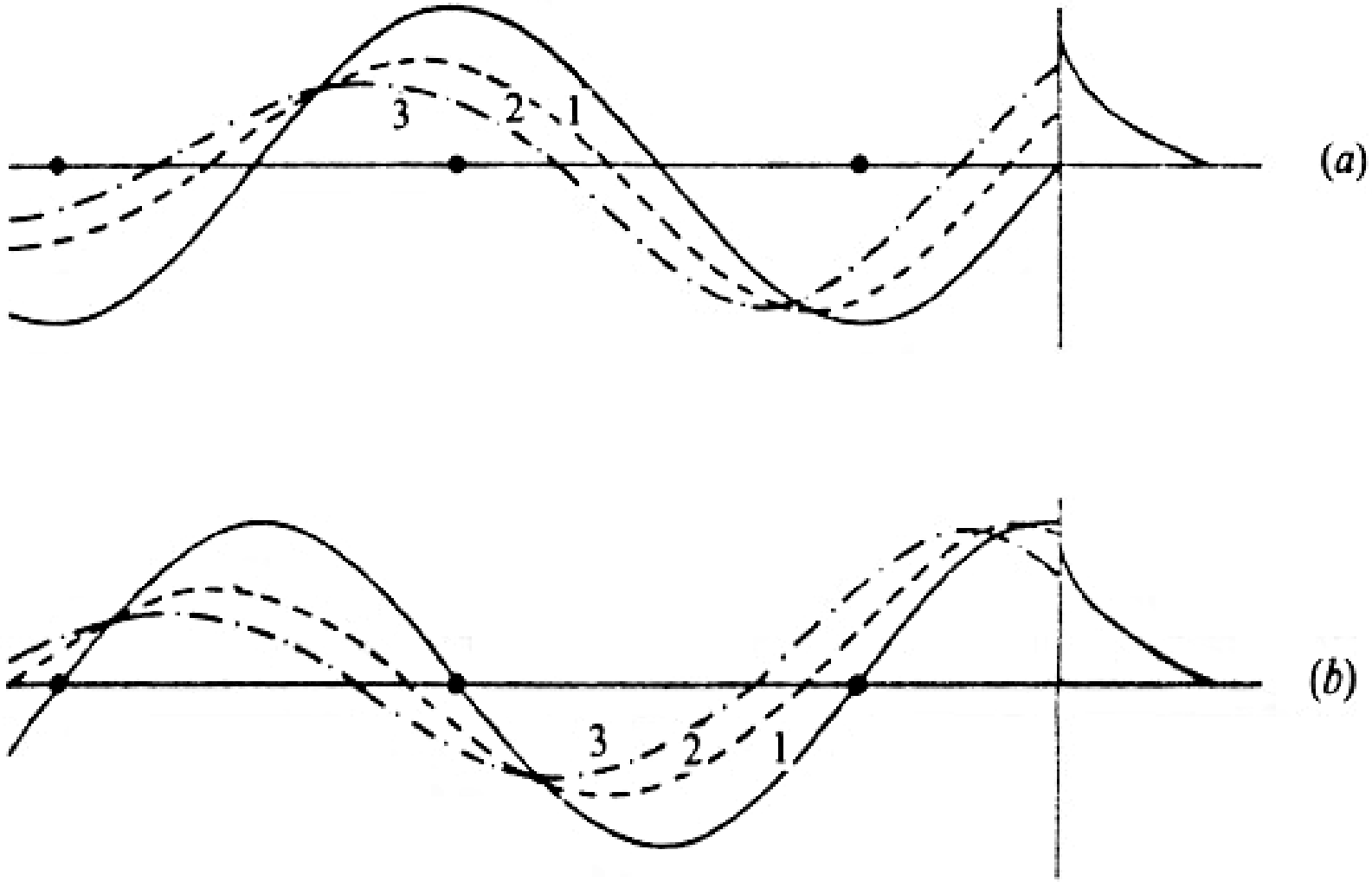

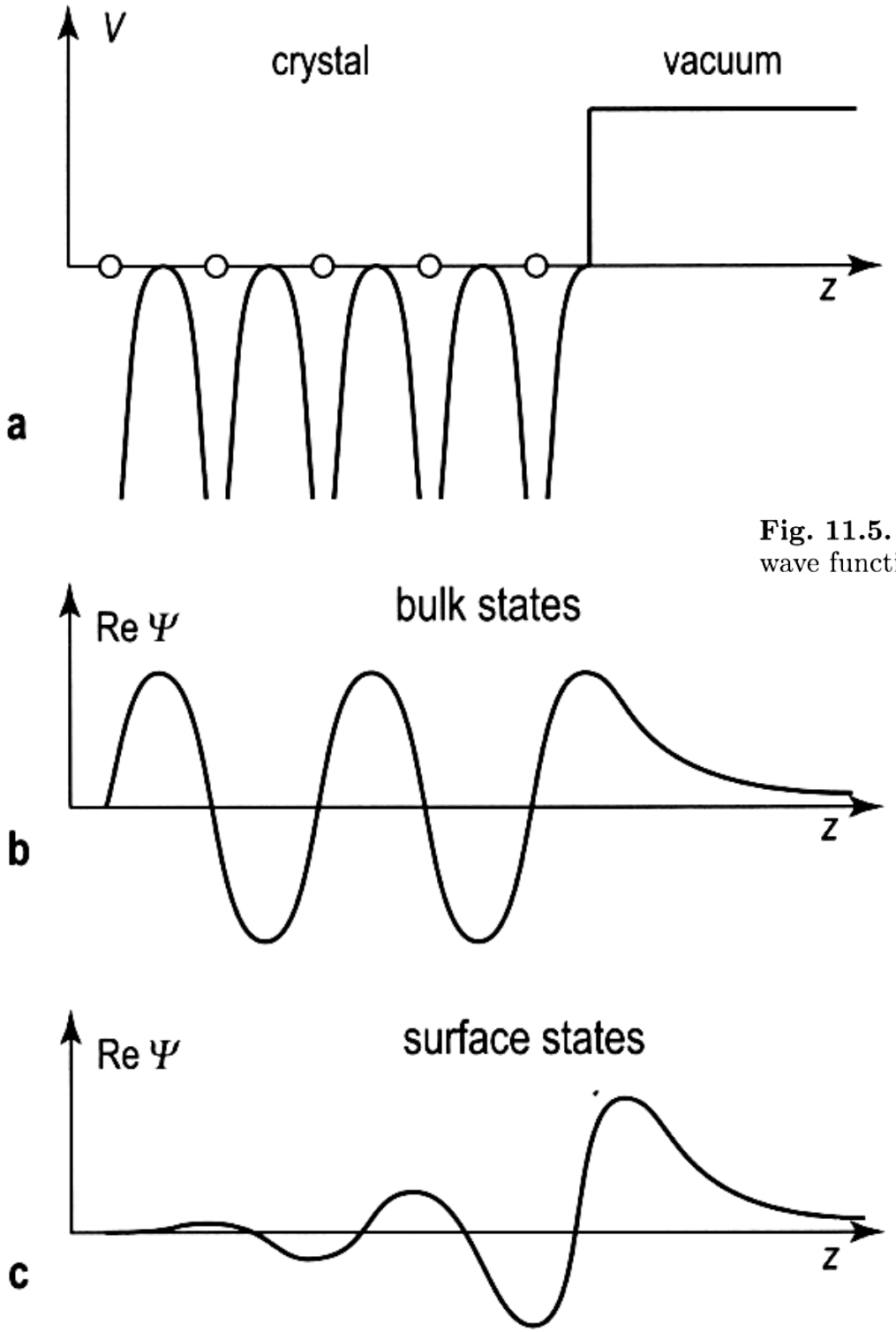

Fig. 11.5. (**a**) One-dimensional semi-infinite lattice model potential. Two types of wave functions of a semi-infinite crystal: (**b**) bulk states and (**c**) surface states

Fig. 4.15. Projected bulk band structure at the surface of a metal. The dispersion of two possible surface state bands is indicated.

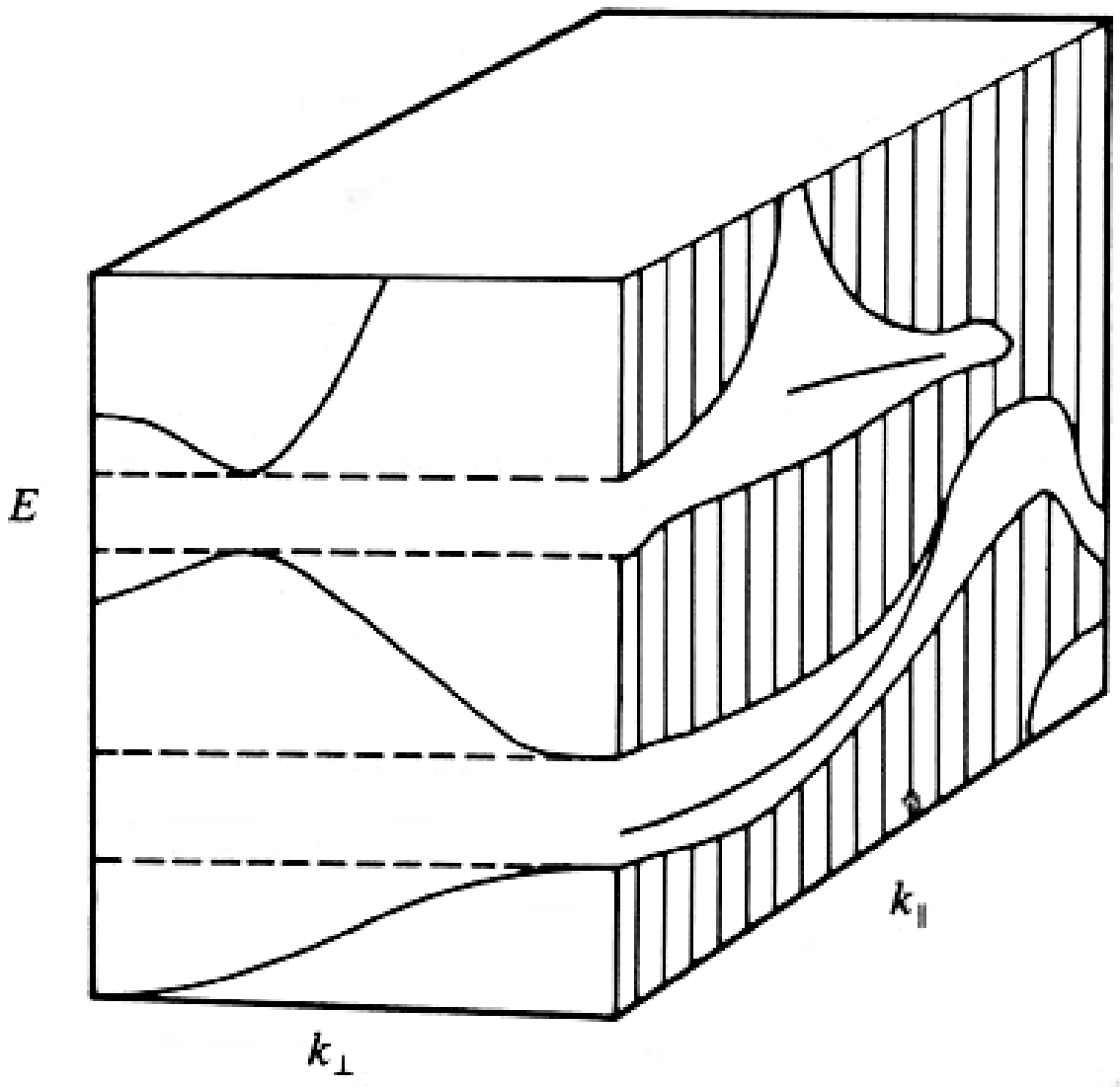

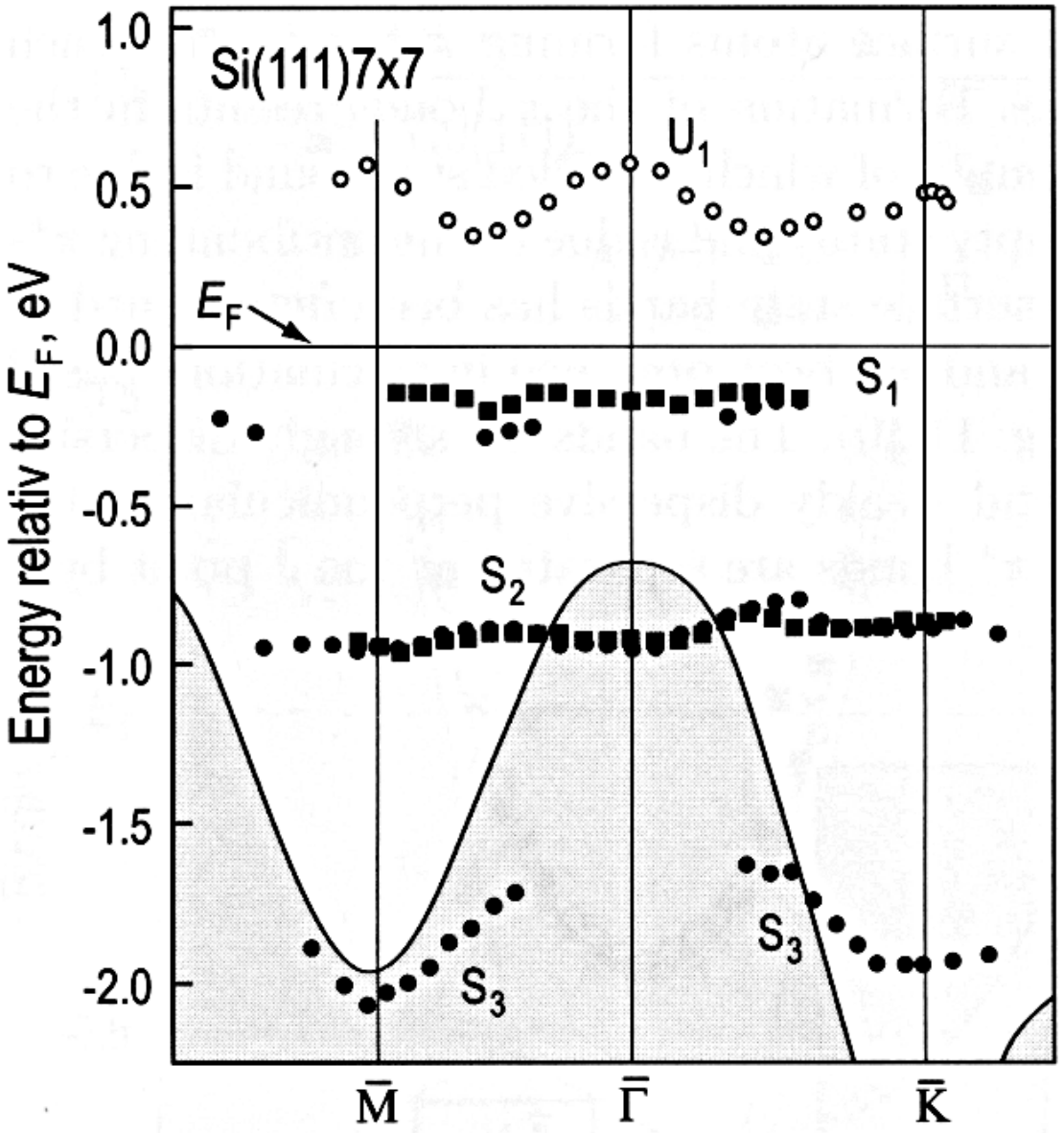

Fig. 11.11. Surface band structure of the Si(111)7×7 surface (referring to the Brillouin zone for the Si(111)1×1 surface) as resulting from ARUPS (closed circles [11.12] and closed squares [11.13]) and KRIPES (open circles [11.12]) measurements. The shaded region is the projected bulk band structure

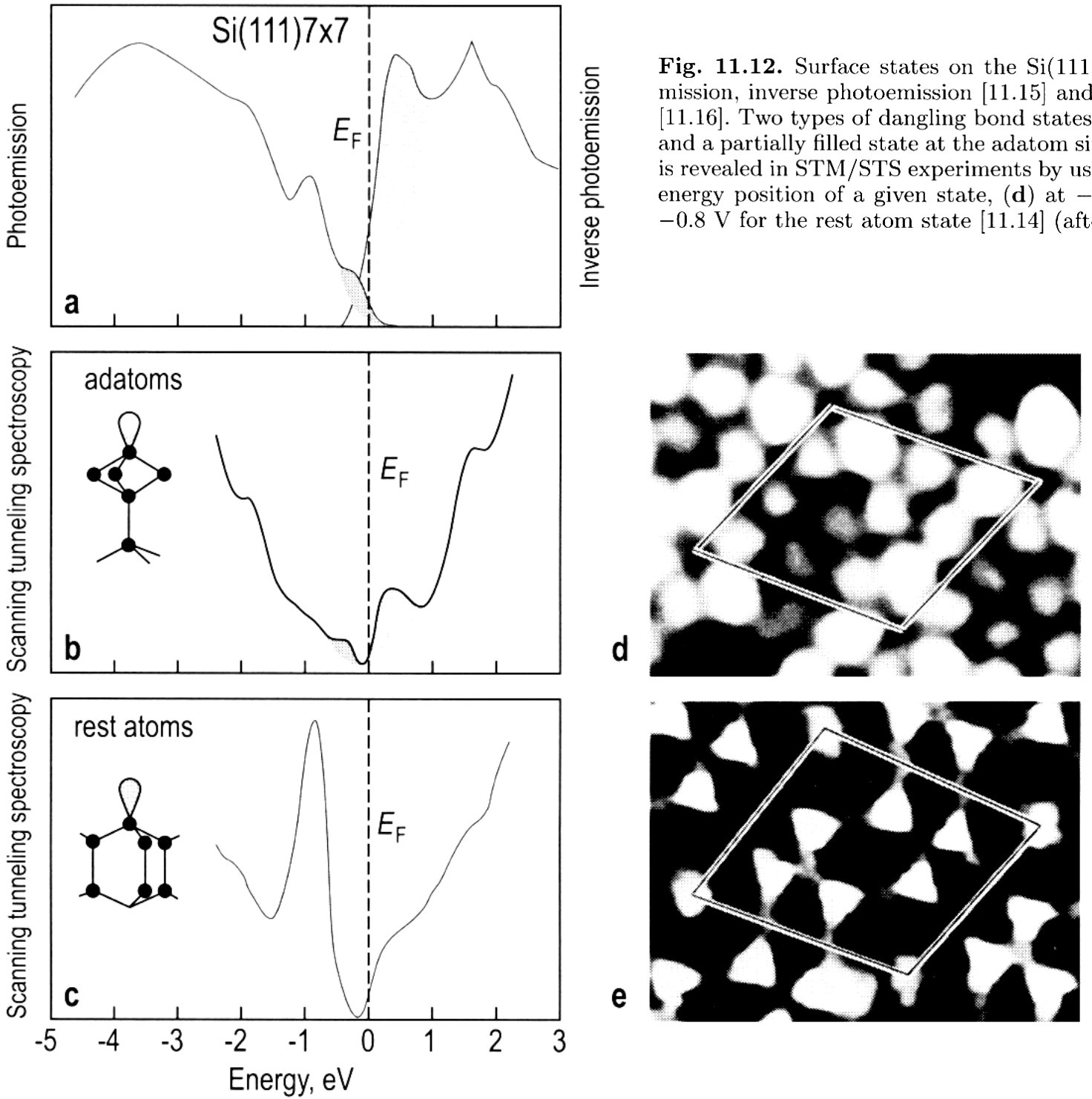

Fig. 11.12. Surface states on the Si(111)7×7 surface detected with (**a**) photoemission, inverse photoemission [11.15] and **b**, (**c**) scanning tunneling spectroscopy [11.16]. Two types of dangling bond states occur; a lone pair at the rest atom sites and a partially filled state at the adatom sites. The surface localization of the states is revealed in STM/STS experiments by using the bias voltage corresponding to the energy position of a given state, (**d**) at −0.35 V for the adatom state and (**e**) at −0.8 V for the rest atom state [11.14] (after Himpsel [11.17])

Slab model

Fig. 4.16. Edge view of a five-layer slab for surface electronic structure calculations. Slab has infinite extent in the x–y plane.

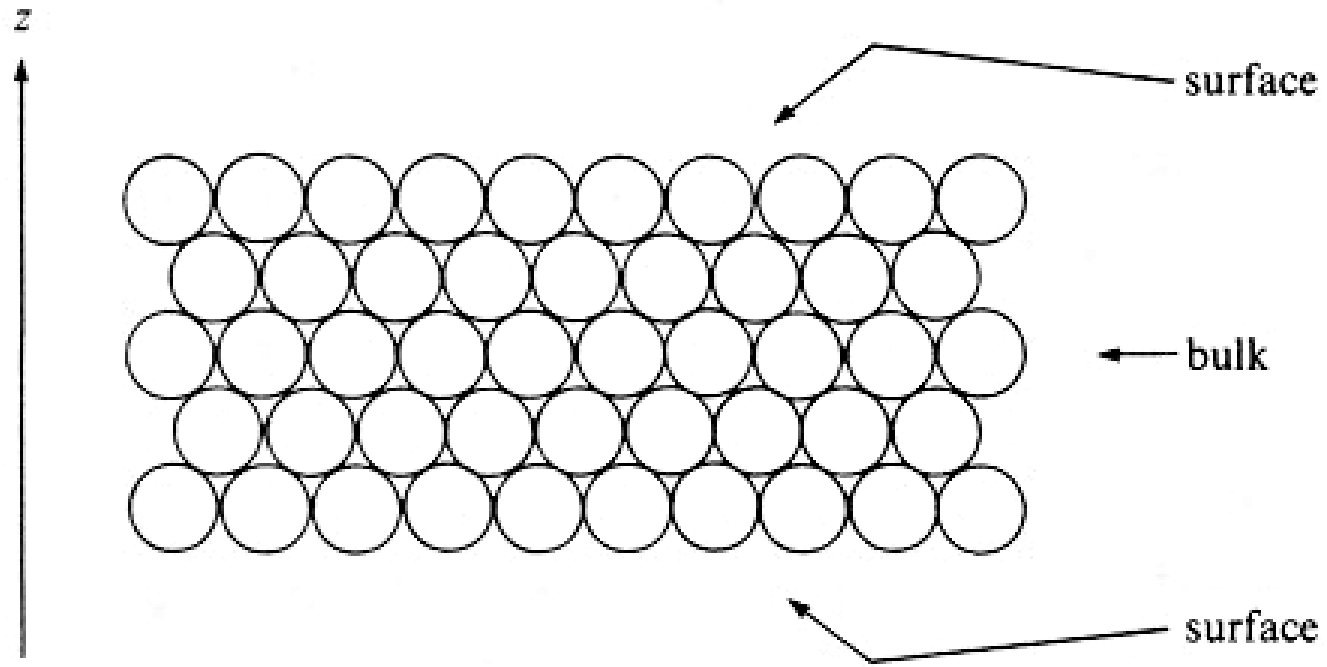

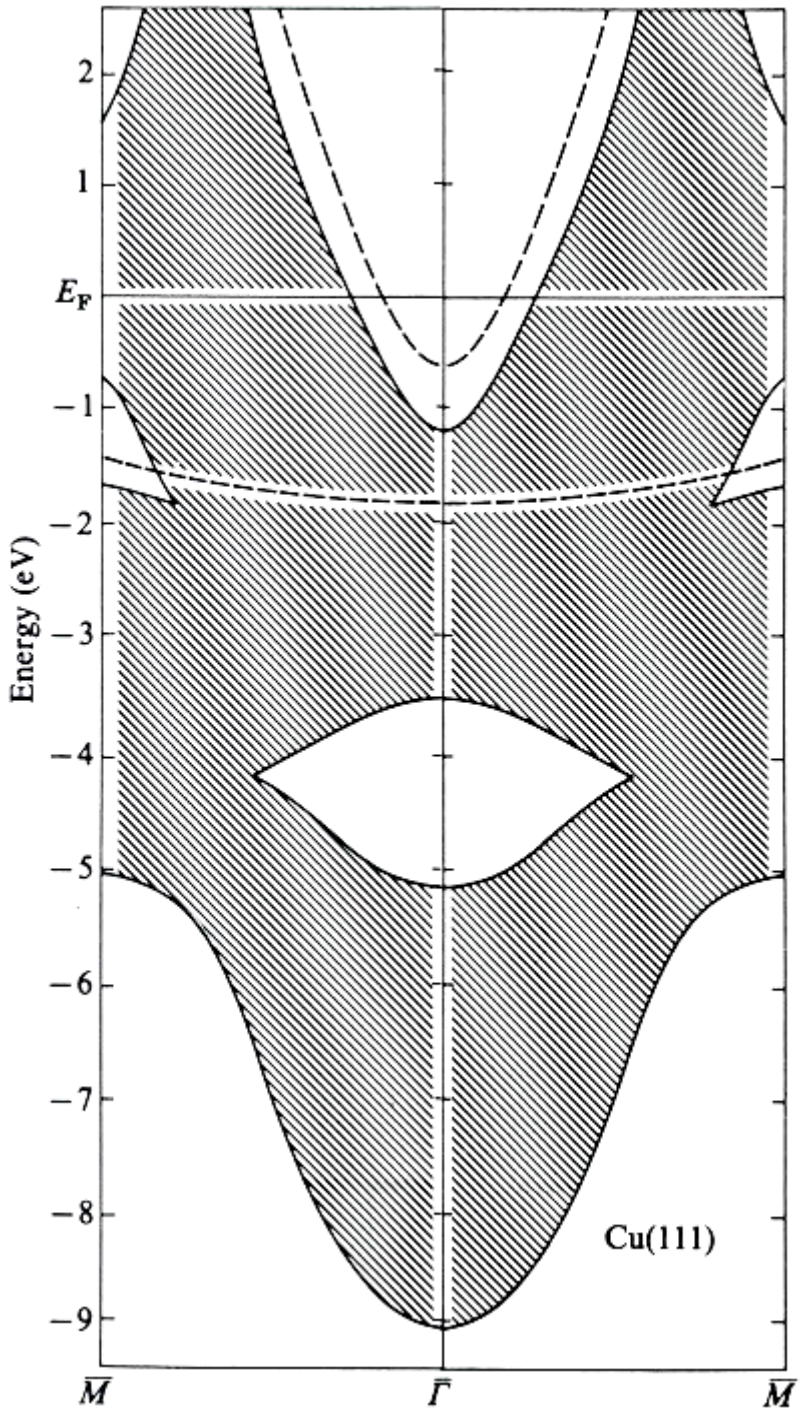

Fig. 4.17. Surface states (dashed curves) and bulk projected bands at a Cu(111) surface according to a six-layer surface band structure calculation (Euceda, Bylander & Kleinman, 1983).

SURFACE STATE WAVEFUNCTIONS

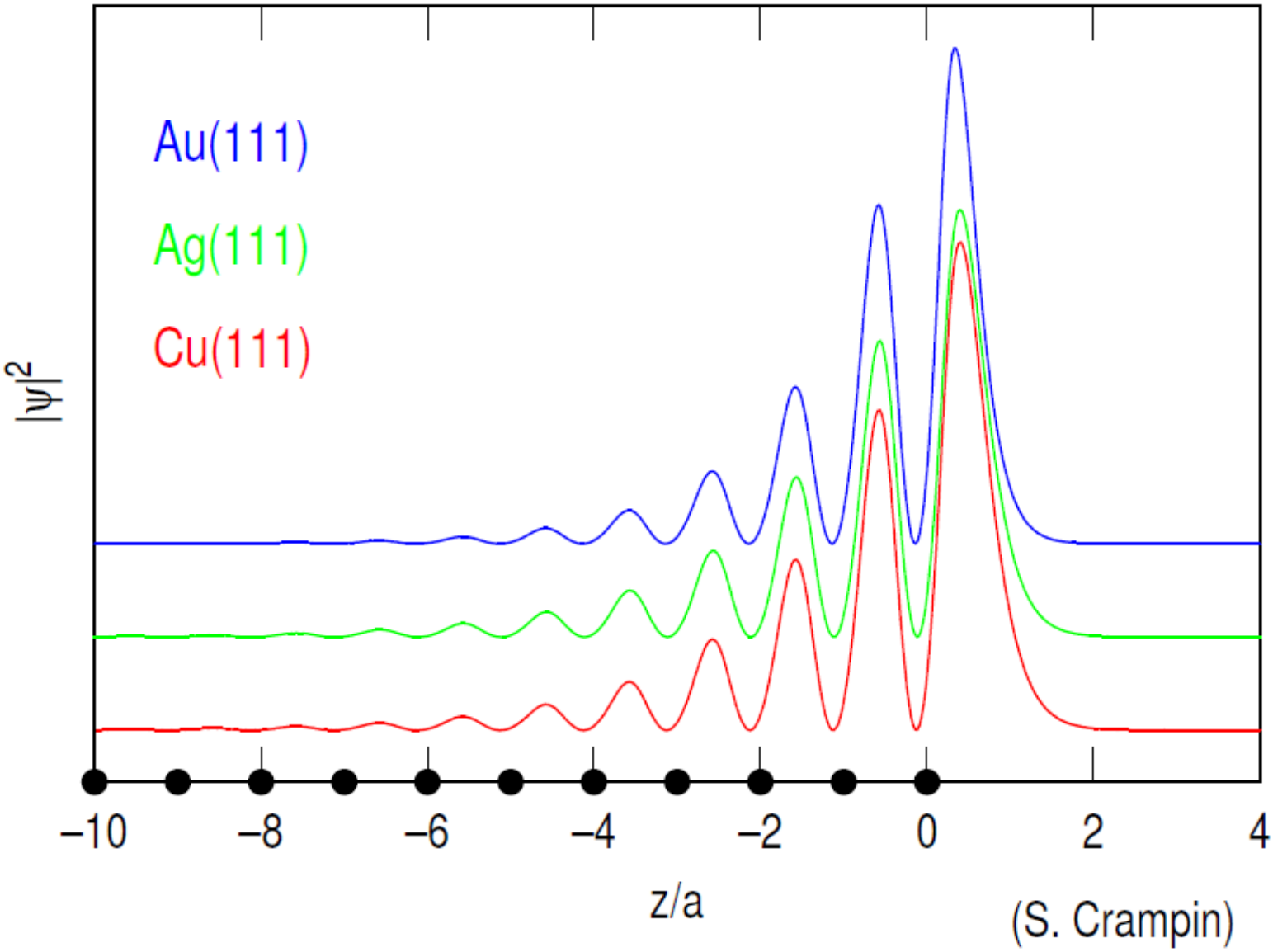

SURFACE STATE WAVEFUNCTIONS

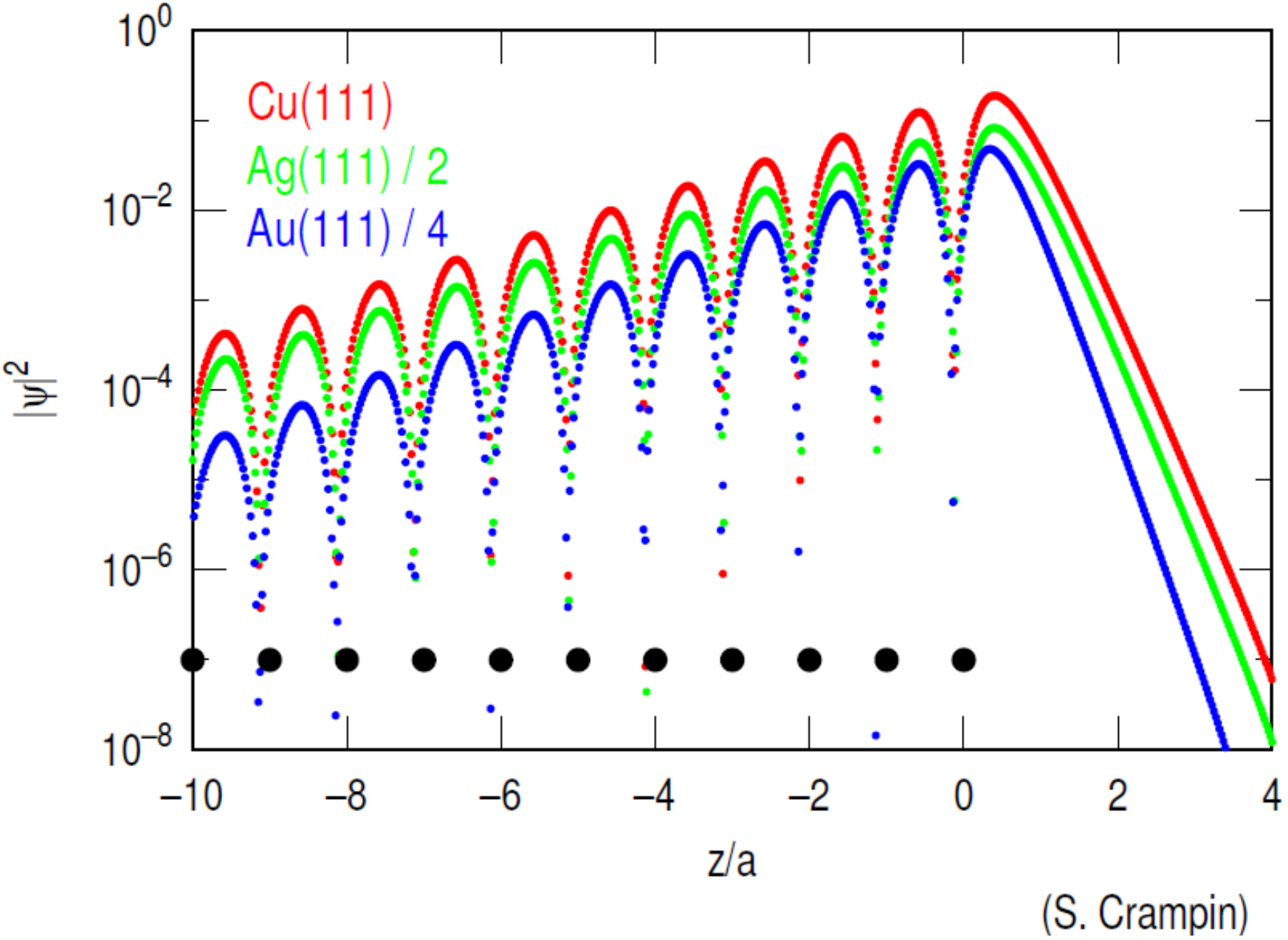

(S. Crampin)

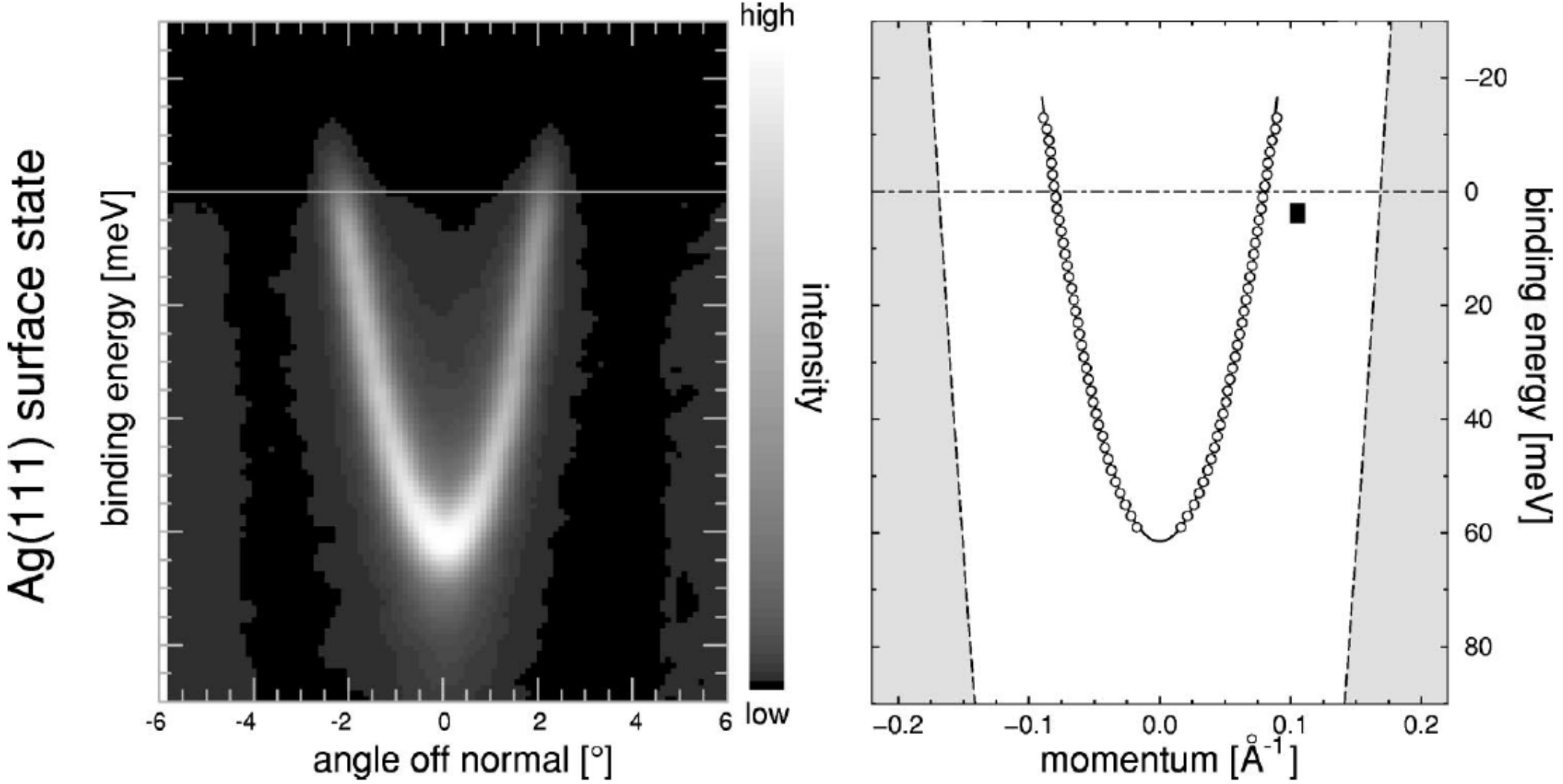

PHYSICAL REVIEW B **63**, 115415 (2001)

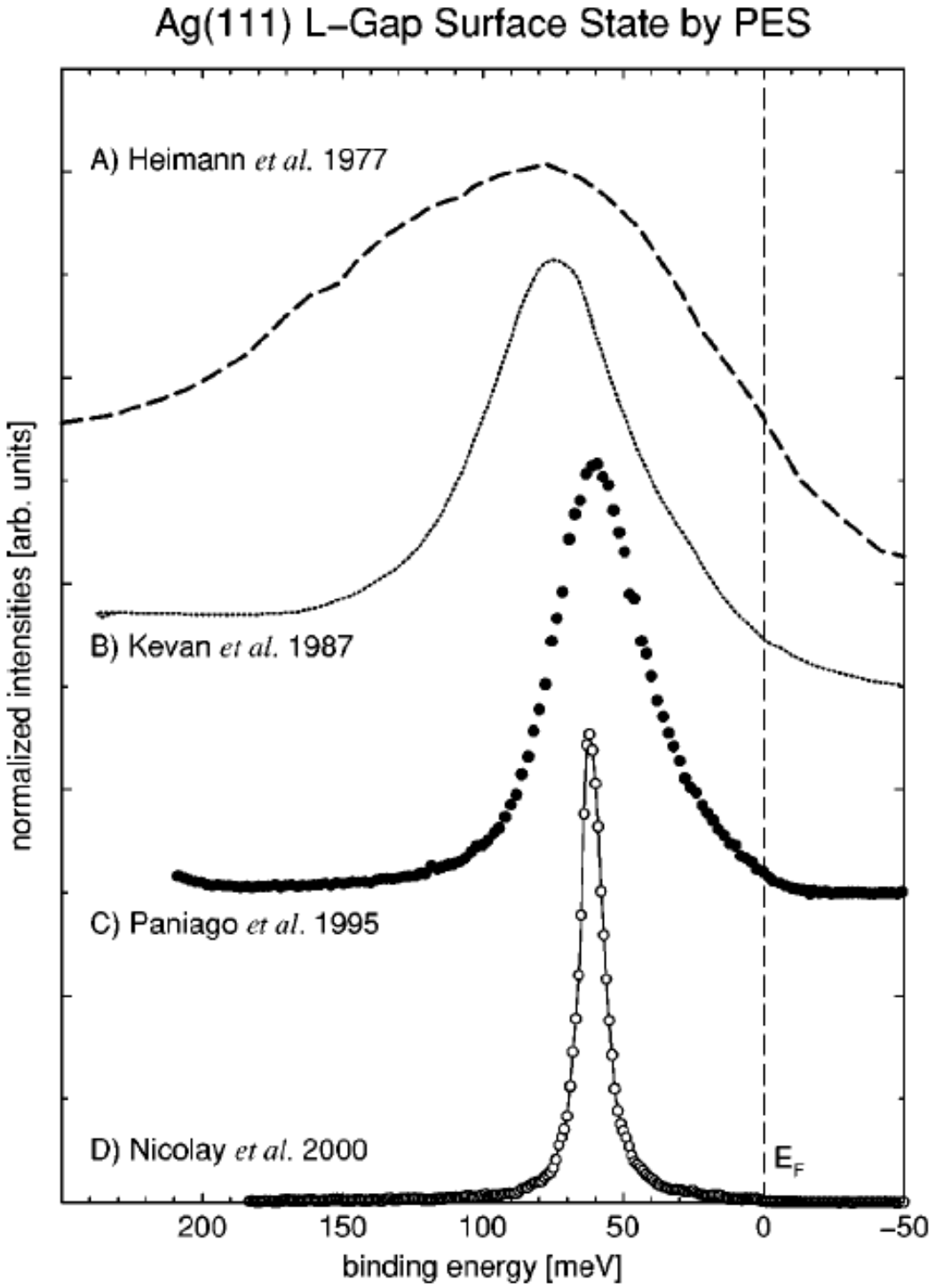
Ag(111) L–Gap Surface State by PES
A) Heimann et al. 1977
B) Kevan et al. 1987
C) Paniago et al. 1995
D) Nicolay et al. 2000
E_F
normalized intensities [arb. units]
200
150
100
50
0
–50
binding energy [meV]

Au(111) surface state

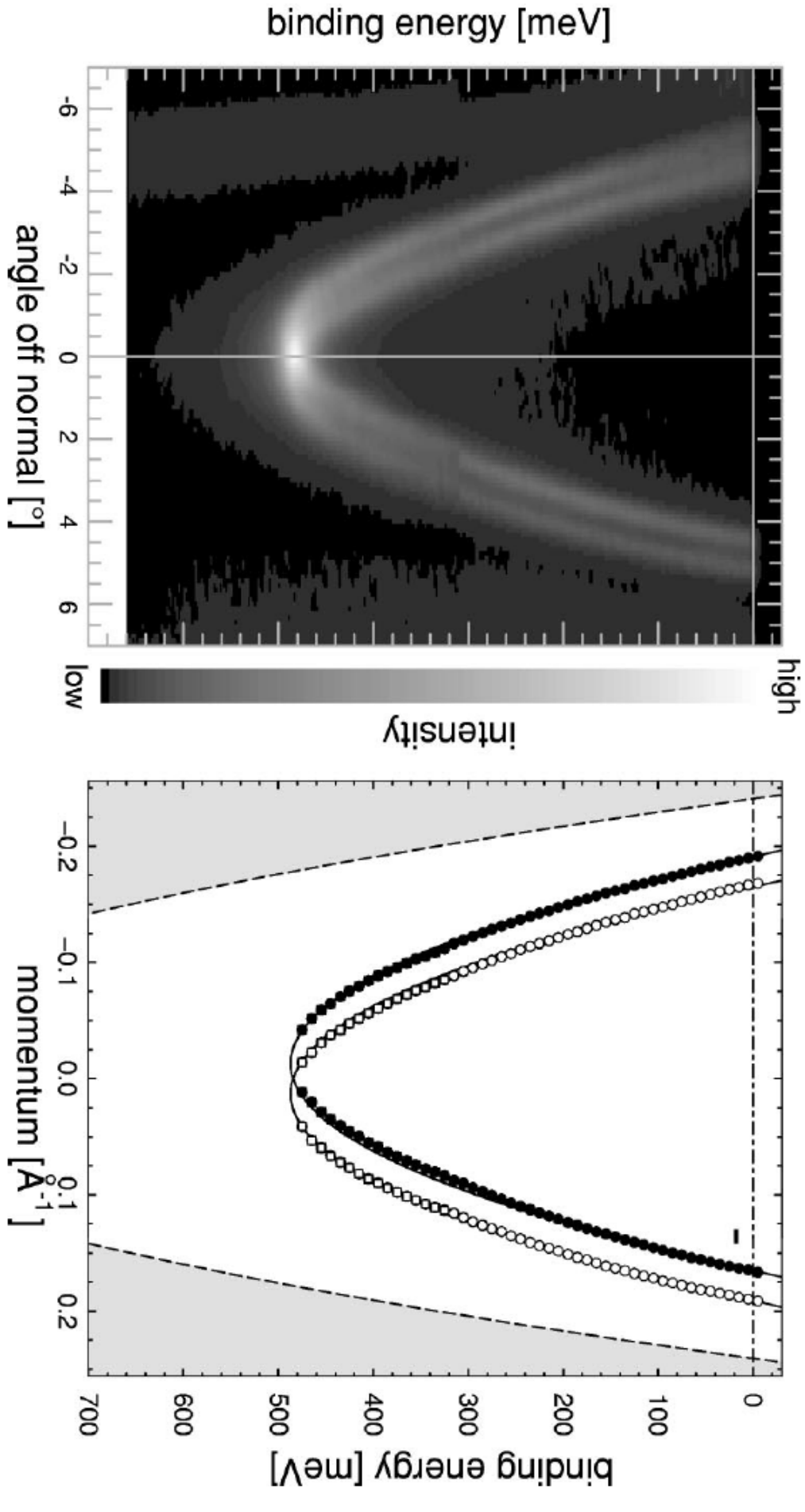

relativistic correction to Schrödinger equation: PRL **77**, 3419 (1996)

$$H_{\mathrm{SOC}} = (\hbar/4mc^2)\,(\nabla V \times \vec{p}) \cdot \vec{\sigma}$$

V: external potential, *p*: momentum, *σ*: Pauli spin operator

approximately proportional to: $\vec{L} \cdot \vec{S}$ **SOC**

→ spin degenerate levels may be spin split by SOC

but: forbidden for systems inversion symmetry

crystal surface breaks this symmetry!

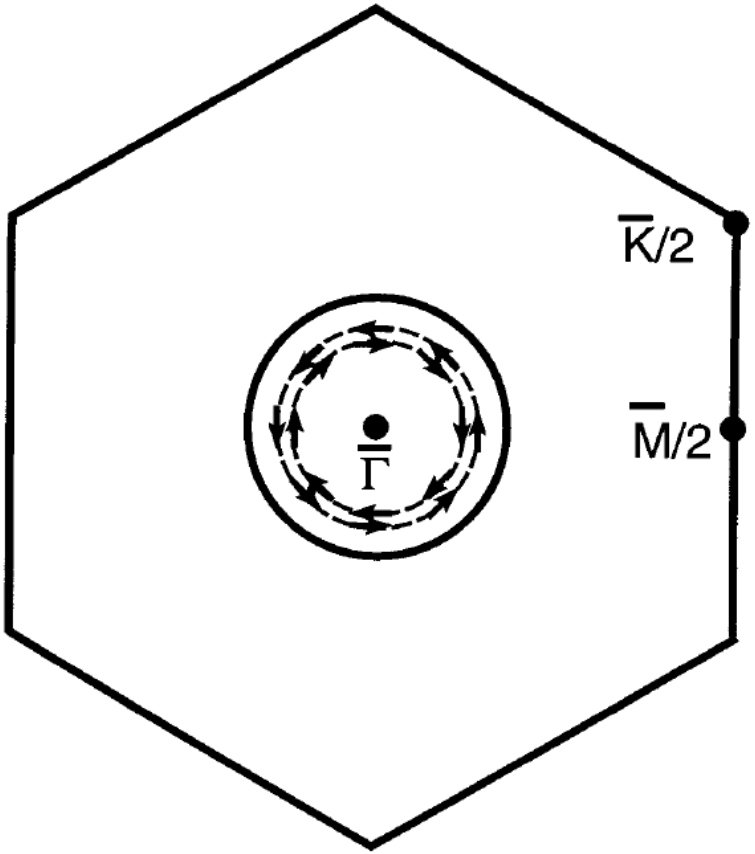

Au(111):

Fermi surfaces and (one half of) the surface Brillouin zone.

Arrows and dashed lines indicate spin orientations

Solid line represents the bulk Fermi surface neck.

All spins are in the plane of the surface.

At the surface: k_F = -0.153, 0.177 Å^{-1}, M = 1.26 Å^{-1}.

In the bulk: k_F = - 0.216 Å^{-1}.

Bildpotentialzustände

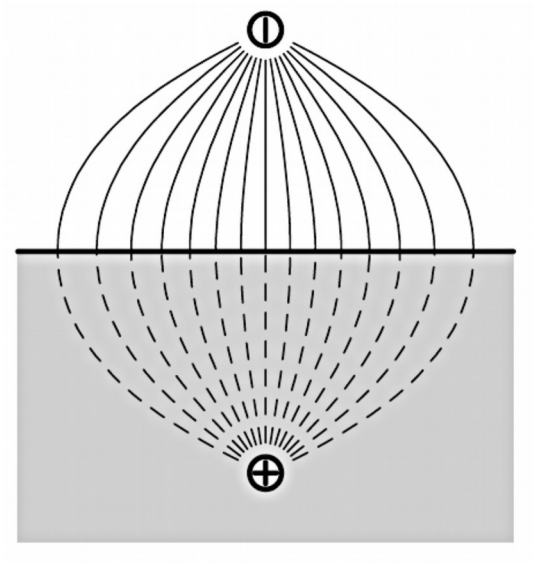

$$E_n = E_{\text{vac}} - \frac{0.85\,\text{eV}}{(n+a)^2}, \quad n = 1, 2, \ldots$$

Aus: U. Höfer, *Dynamik von Bildpotentialzuständen*

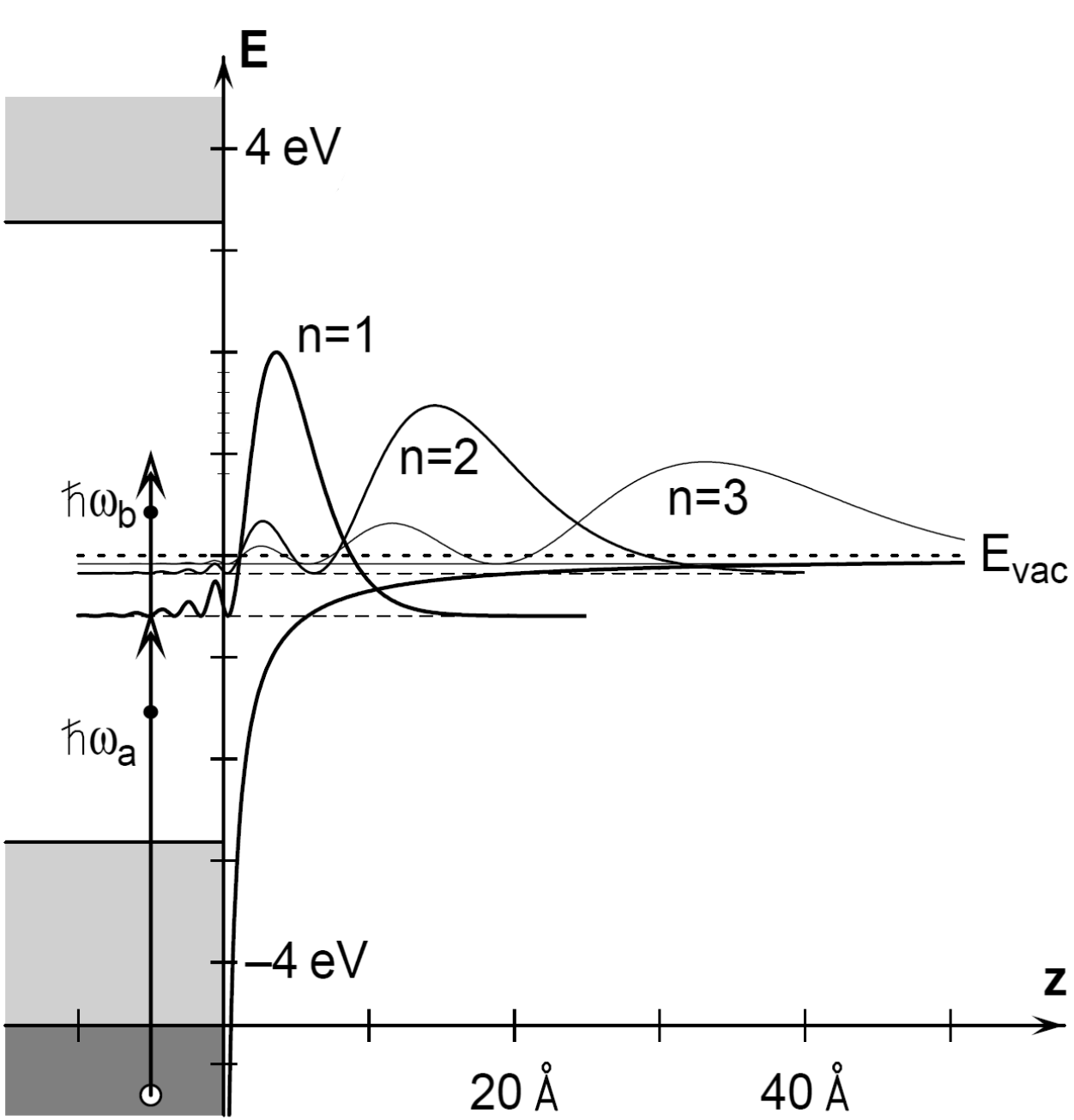

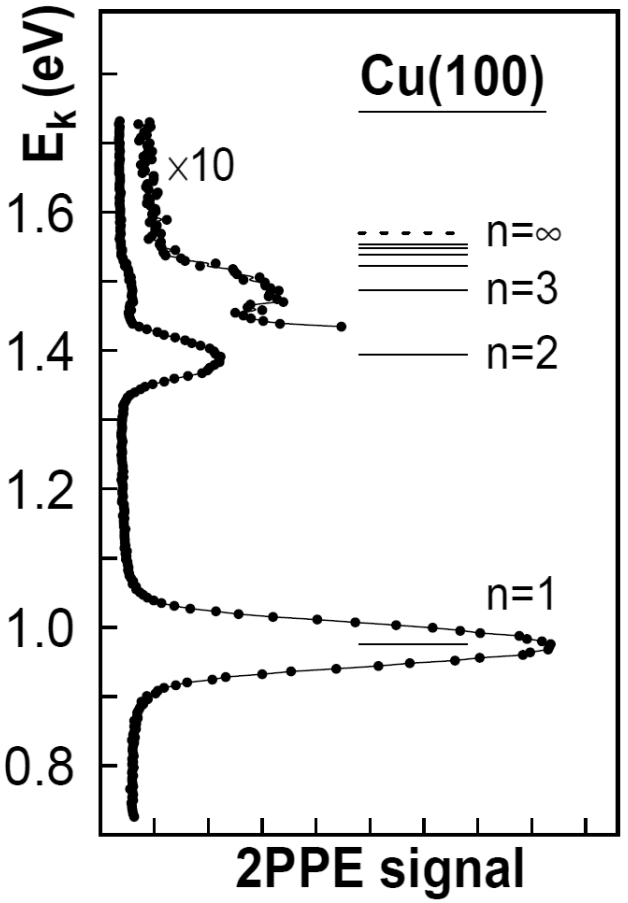

Photoelektronen-Spektrum
Aufgrund sequentieller
Anregung mit Photonen der
Energien hv_a und hv_b

Aus: U. Höfer, *Dynamik von Bildpotentialzuständen*

Zweiphotonenphotoemission (2PPE)

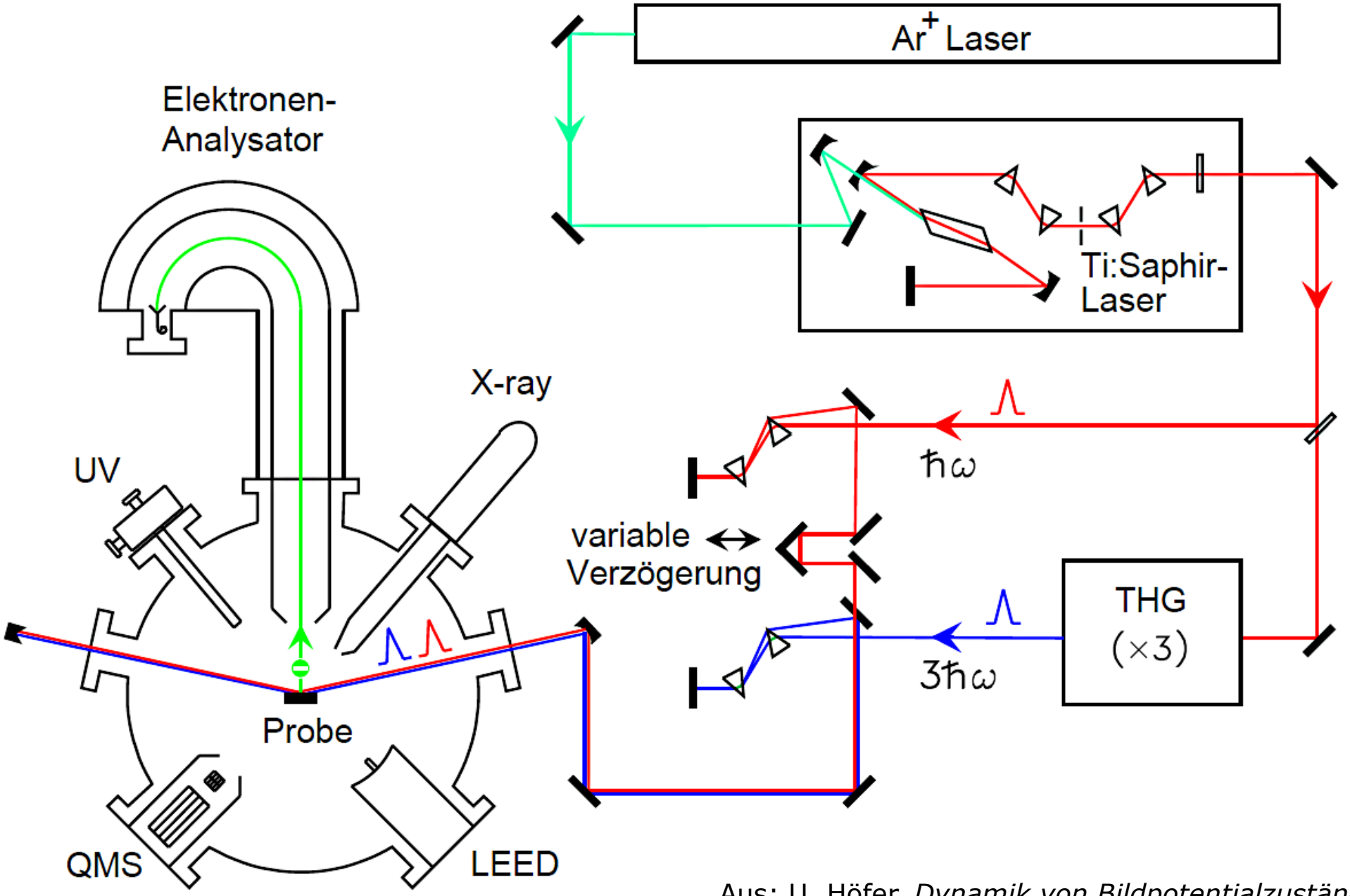

Aus: U. Höfer, *Dynamik von Bildpotentialzuständen*

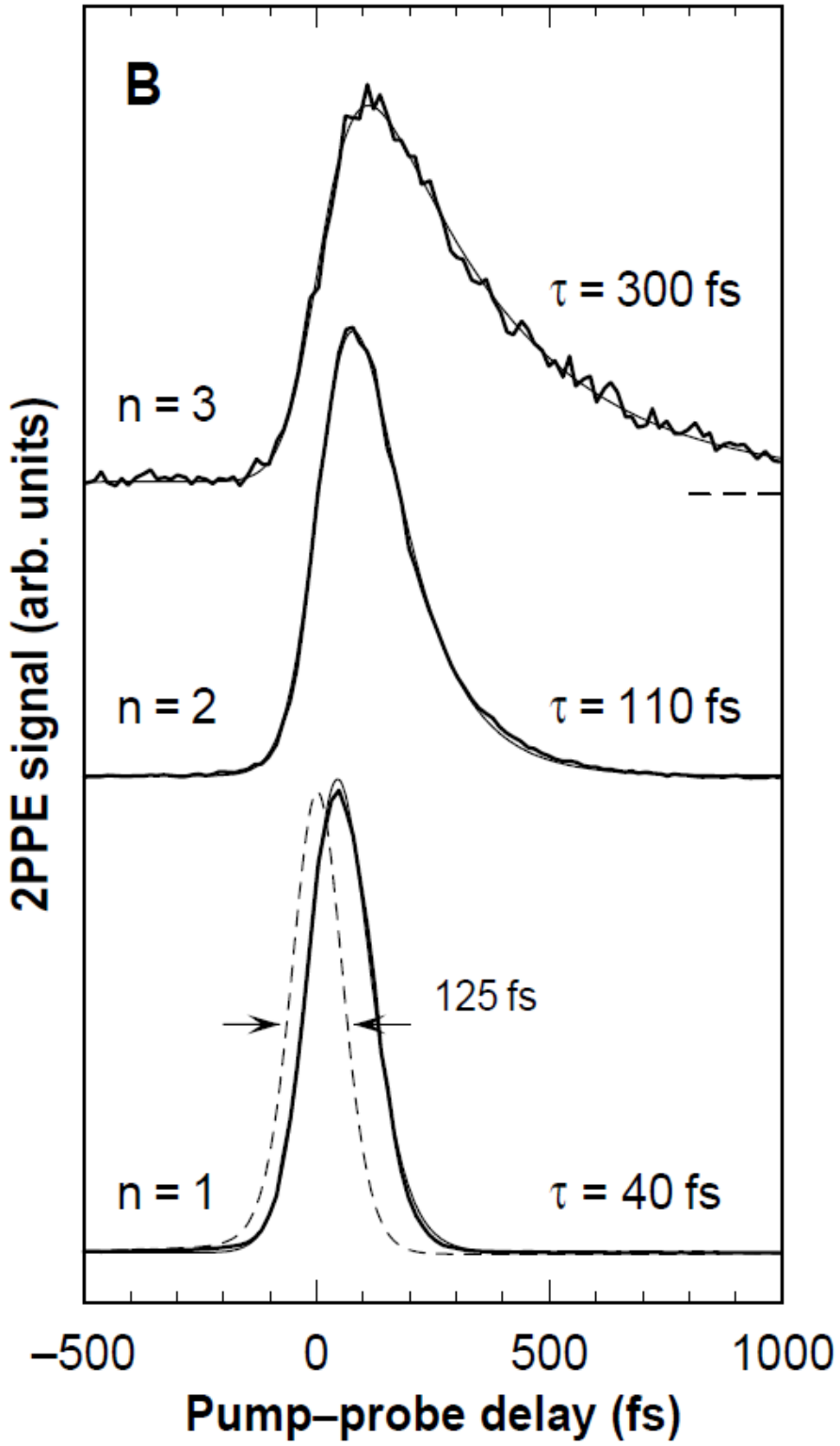

Cu(100)

$E_B > 80$ meV

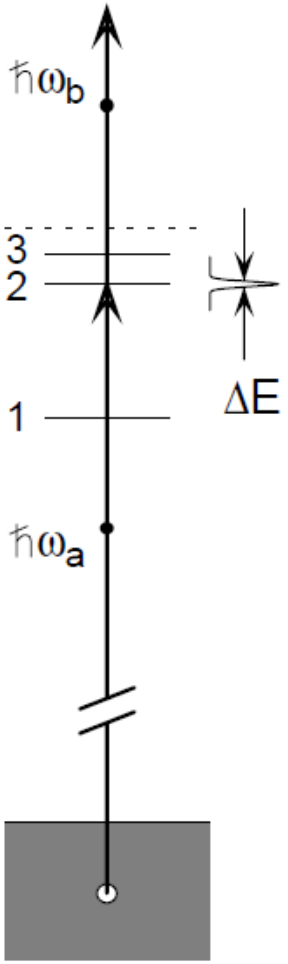

Zeitabhängigkeit des 2PPE-Signals der niedrigsten drei Bildpotentialzustände von Cu(100).

Gestrichelte Linie: Kreuzkorrelation der Pump- und Probeimpulse ohne resonante Zwischenzustände.

Die geringe spektrale Breite ΔE der Pumpimpulse auf der Energieskala der Bildpotentialzustände verdeutlicht das Anregunsschema rechts.

Aus: U. Höfer, *Dynamik von Bildpotentialzuständen*